5-16-2013

# Towards a characterization of wetland invasive vegetation using a combination of field and remote sensing techniques

Nicole Dutcher

**Towards a Characterization of Wetland Invasive Vegetation Using a Combination of Field and Remote Sensing Techniques**

**By Nicole M. Dutcher**
B.S. Rochester Institute of Technology 2009

Rochester Institute of Technology
College of Science
Thomas H. Gosnell School of Life Sciences
Program in Environmental Science

A thesis submitted in partial fulfillment of
the requirement for the degree of
Master of Science

Approved May 16th 2013

by:

_____
Anna Christina Tyler, Ph.D.
Co-chair of Committee

_____
Jan van Aardt, Ph.D.
Co-chair of Committee

_____
Karl F. Korfmacher, Ph.D.

## TABLE OF CONTENTS

# TABLE OF FIGURES, TABLES AND EQUATIONS

## ACKNOWLEDGEMENTS

Financial support for this study was provided by an Alumni Student Research Grant, awarded through the Thomas H. Gosnell School of Life Sciences at Rochester Institute of Technology. I am very grateful for the continual support of my parents and friends throughout my research and studies. I would also like to thank my professors for their constant support and input throughout my graduate career, specifically Dr. Christy Tyler, Dr. Jan van Aardt and Dr. Karl Korfmacher. Thanks are also due to Dr. Tyler's, Dr. Korfmacher's and Dr. van Aardt's research labs from 2011 to 2013 for their help in field sample collections, as well as their continual feedback and support.

## ABSTRACT

Creation of compensatory wetlands has been required in the U.S. since the late 1980s in an attempt to offset the massive decline in freshwater wetlands. To meet permitting requirements, vegetation composition in mitigation wetlands must be monitored for a minimum of five years following creation. Unfortunately, mitigated wetlands often lack the functionality of natural wetlands and may form hotspots for invasive plant species. However, wetland assessment is a time-consuming process that may also disturb fragile nascent plant communities. Thus there is a need for approaches that minimize disturbance, but still enable the collection of data over large portions of the landscape. Remote sensing, using hyperspectral imagery augmented by field data collection is a potential tool for rapid ecosystem assessment. In July 2010, vegetation community composition, spectral signatures of individual plant species, and plant canopies, and an aerial hyperspectral imagery dataset were obtained from two natural and two mitigation wetlands on the Rochester Institute of Technology (RIT) campus, Rochester, NY. We were able to locate specific wavelengths for four invasive plant species spectra that can be used to classify and map these species on the RIT campus with an overall accuracy of 94.34%. Reed canarygrass had a higher reflectance than the other three species and differences along the red-edge and near-infrared regions also enabled differentiation between broadleaf cattail and narrowleaf cattail. Values within the blue, red, red-edge, and near-infrared regions are needed to create a multi-spectral sensor with a larger emphasis on the red-edge and near-infrared regions. Such a sensor would be more readily available for land managers for classification and analysis of large plots of land, limiting the amount of time, personnel and funding needed to process the imagery and allowing managers to more rapidly identify patches of invasive plant species with minimal intrusion on sensitive wetland environments.

## INTRODUCTION

Wetlands provide numerous ecosystem functions and services, including carbon sequestration, heavy metal reduction, sediment and pollutant removal, floodwater storage, groundwater recharge, and habitat for both resident and migratory organisms (National Research Council 2001; Kent 2001; Zedler and Kercher 2005). However, wetlands face a wide range of disturbances that impact their functionality and usefulness in terms of the ecosystem services they provide.

There has been greater than a 50% decline of wetlands in the United States (U.S.) in the last 200 years, with the largest loss occurring to freshwater emergent wetlands primarily due to rural development and infrastructure (Dahl 1986; Dahl 1990). Specifically, 60% of wetlands in western New York were destroyed by the 1980s due to suburban sprawl (Niagara Frontier Wildlife Habitat Council 2013). Prior to the 1970s, there were no regulations in place in the U.S. to protect wetlands and maintain the ecosystem services that they provide (Dahl 1986). In 1972, wetland modification and loss became regulated under Section 404, of the Federal Water Control Act, also known as the Clean Water Act (CWA). Section 404 requires developers and landowners to obtain a permit prior to dredging or filling in navigable waters and adjacent wetlands (Clean Water Act 1972). Today, the U.S. Army Corps of Engineers (USACE) is responsible for issuing permits under Section 404 for the authorization of dredging or filling of U.S. waters and adjacent wetlands; and the U.S. Environmental Protection Agency (EPA) has legislative authority to deal with unpermitted dredge and fill activities (Clean Water Act 1972). In addition New York State (NYS) passed the Freshwater Wetlands Act (1975) to more specifically protect and conserve wetlands found in NYS for the general welfare of wetlands but

also with the purpose to benefit the state economically, agriculturally and socially ("New York State Wetlands Assessment (Section 305(b))" 2005).

Since the late 1980s compensatory wetlands for the purpose of wetland mitigation have been the primary method for reducing wetland losses in the U.S. (Dahl 1990). If altering or destroying a wetland is unavoidable for a project, approval may be contingent on minimizing the impact in conjunction with restoring, enhancing, or creating wetlands to make up for this unavoidable loss (Brinson and Rheinhardt 1996). This is the idea of no-net loss, where through the approval of a permit to alter or destroy a wetland, land managers must develop a plan to make up for the loss in either wetland area or function. These permits require compensatory mitigation to fulfill the no-net loss policy, which typically is comprised of restoration, enhancement, or creation of a wetland, or any combination thereof (Brinson and Rheinhardt 1996; Zedler 2004).

When a permit is issued, a mitigation plan is also created for the site. The USACE currently requires five years of monitoring after mitigation is complete to ensure that the management plan is being followed and is successful (Brinson and Rheinhardt 1996; Zedler 2004). Management plans for mitigated wetlands are generally structured based on the reference standards or variables of naturally occurring wetlands that the mitigated wetlands are being modeled after.

A large concern with mitigated wetlands is that the general process can create a primary and secondary succession process in the area with a great concern that invasive plant species will colonize the area first and native plants will not be able to get established (Zedler 2004; Zedler and Kercher 2005). In this research study, invasive species are considered to be any species that

are un-wanted in the wetland. Invasive plants can influence the drainage patters and functions that the wetland is supposed to be performing for the ecosystem. For wetlands the most common destructive invasive plants are grasses and reeds that create monoculture stands which reduces the flow of water throughout the wetland, and in turn do not allow a consistent in-flow and out-flow of water; they also limit the wetlands ability to act as a groundwater recharge zone and limits its ability to remove harmful pollutants and sediment from the surface and groundwater; as well as monoculture stands limit the biodiversity of an area which in turn limits the amount of habitat that the area can provide for migratory organisms and endangered species. Many mitigation plans therefore involve showing a decline in surface coverage of invasive species over time (U.S. Department of the Army 2009); or the permit might require that the mitigated wetland contain less than a specific percent coverage of all invasive species present. In order to show that the goals of the mitigation plan are being met, an extensive amount of field monitoring is needed.

Because of the large number of mitigation wetlands currently in the U.S., there is a need to assess their state and function in comparison to natural wetlands to determine if they have functional equivalence (Haslam 2003; Balcombe et al. 2005). Assessing the status and health of various components of a wetland, including water quality, plant species composition, soil characteristics, and nutrient concentrations can help to determine if a mitigation wetland is performing the way it was intended to (Brinson and Rheinhardt 1996; Zedler and Kercher 2005). One important indicator of wetland function is the plant community structure, since vegetation plays a distinct role in the identification of wetlands and the services that they provide. Wetlands with greater structural diversity maintain greater wildlife species diversity/biodiversity (Balcombe et al. 2005). Further, the plant species and communities present are indicators of the water regime and animal communities present (Haslam 2003). Different plant species

combinations have been found to be dominant depending on the water level, anoxic conditions, soils present, and nutrients present in the wetland (Haslam 2003). Individual plant species typically have an optimal range of nutrient availability, such that measures of plant community composition may be indicative of the local nutrient regime (Haslam 2003). Vegetation thus is a key identifier to what type of wetland it is and what services the wetland can provide, because of this the NYS Freshwater Wetlands Act of 1975 uses vegetation as its basis for identifying wetland communities (Huffman & Associates 2000; "New York State Wetlands Assessment (Section 305(b))" 2005).

The vegetative matrix of a wetland can be classified into three distinct groups; mixed species wetland community, vegetation monoculture of native species, and monocultures of invasive species; the type of vegetation matrix that would be considered favorable for a wetland depends on what type of wetland it is, and the location and function it provides. With an understanding of the different plant communities that are present in a wetland, a baseline can be established of what is currently growing in natural wetlands and what should be expected to grow in created/mitigated wetlands (Barona et al. 2003). With this baseline information, vegetation in a mitigated wetland can be compared to similar natural wetlands found in the same geographic region to see if they have the same vegetation types. If a mitigated wetland has a different vegetation matrix compared to the reference wetland it was modeled after, then the mitigation is not complete according to the permit and the wetland is not performing the functions it was designed to for the ecosystem.

The collection of field data to assess wetland health is time consuming and requires funding and resources (Adam et al. 2009). In addition, frequent field monitoring collection creates the risk of disturbing fragile wetland communities. However, with novel technology there

are a wide variety of ways to assess the health and stability of an ecosystem without the need for disruptive field sampling (Brinson and Rheinhardt 1996; Haslam 2003; Adam et al. 2009). A method with high potential for success is through the use of remote sensing techniques, typically hyperspectral imagery, combined with more limited field data collection (Lyon 2001). Remote sensing provides a practical and economic method for mapping and monitoring vegetation species and biogeochemical distribution, quality, and quantity within a geographic region (Adam et al. 2009).

Hyperspectral imagery, also known as imaging spectroscopy, is a relatively new tool within the realm of remote sensing. It differs from other remote sensing approaches, such as multi-spectral imaging, because it measures the reflective radiance from the surface of the Earth in contiguous bands of narrow wavelengths (10-20 nm) over a broad spectral range (350-2500 nm) (Hall 2004; Adam et al. 2009). Since it spectrally oversamples the landscape, the image contains an enormous amount of detailed spectral information. For environmental analysis, the most common method for collecting hyperspectral data is with airborne sensors, because they provide more detailed images due to the high spatial resolution, which in turn has been shown to be more efficient when mapping wetlands than compared to satellite imagery (Artigas and Yang 2006; Adam et al. 2009). This allows hyperspectral imagery to be a great tool for short term studies or glimpses at landscapes at a specific period of time, but may not be deal for long term studies since it is costly to run multiple data collection flights (Adam et al. 2009).

Hyperspectral imagery was originally developed as a tool for the detection of potential oil fields, as well as for mining, given its ability to discriminate between specific minerals. As public accessibility to data has increased over the past few decades, its use and application has spread into other fields. Biologists and conservationists have now begun to use imagery for

detecting crop health, productivity and monitoring stress symptoms to prevent the early spread of diseases in agriculture crops (Lacar et al. 2001; Shippert 2004; Manjunath et al. 2011). This idea can also be extended to the field of ecology and landscape management to assess the health and functionality of an ecosystem (Hall 2004; Yang 2005; Artigas and Yang 2006; Siciliano et al. 2008; Cho et al. 2009).

Hyperspectral imaging therefore has become a favored sensing approach, because it can distinguish more clearly between materials that are spectrally similar within the landscape when compared to multi-spectral imagery, and is able to detect subtle differences along patch edges and mixed vegetation types (Jollineau and Howarth 2008; Manjunath et al. 2011). For example, studies have shown that, while multi-spectral imagery is able to classify vegetation types, hyperspectral imagery is able to discriminate more clearly between similar vegetation groupings or species (Adam et al. 2010; Artigas and Yang 2006; Cho et al. 2009). Underwood et al. (2003) also showed that hyperspectral imagery is useful for detecting small patches of invasive plant species, where multi-spectral was only able to detect larger monocultures.

This powerful approach is possible because each plant species theoretically has a unique spectral signature and can be differentiated from one another, with the largest differences in the visible and near-infrared (VNIR) wavelength regions, expressed through specific absorption characteristics (Barona et al. 2003). The visible spectrum is dominated by pigments within leaves and soil, the red-edge displays rapid change in chlorophyll levels, the near-infrared is dominated by vegetation cell structure, and the shortwave-infrared region is sensitive to the variations in moisture content of the atmosphere, soil and vegetation (Adam et al. 2009). Through a comparison of images, various studies have shown that there are a few specific bands within each wavelength region that are useful when trying to discriminate among species and map

landscape characteristics, as well as ecosystem health (Appendix 1). For example, while mapping salt marsh vegetation types in New Jersey meadowlands, Artigas and Yang (2006) used the spectral differences along the red-edge and in the near-infrared region to discriminate among visibly similar species, such as *Spartina alterniflora, Spartina patens, Phragmites australis* and *Distichlis spicata.* By mapping the spectra of vegetation, we can potentially get an idea of useful spectral shape (slope and "curvature") or bands for various canopy groupings and species, ultimately aiding in the differentiation of species. Because of the vast amount of information gained and the non-intrusive nature of the sampling, hyperspectral imagery has great potential as a useful mechanism for determining wetland ecosystem structure and function.

Through the development of a model or matrix of what common vegetative plant communities are found in wetlands in western New York State and their plant signatures, a spectral library can be developed for specific species (Schmid et al. 2004; Zomer et al. 2009). This information can then be used for similar known wetlands in New York State to assess the vegetative structure to ease monitoring, management, and restoration efforts in the future. At present, there is not a standard spectral library for vegetation types or species (Zomer et al. 2009), especially wetland species due in part to the fact that spectral signatures of vegetation, even for a single species, changes throughout the seasons, as they mature, and in different regions of the globe (Barona et al. 2003; Artigas and Yang 2006; Zomer et al. 2009). However, regional or local spectral libraries are useful because they contribute to describing the distribution of various species and vegetation types within a specific area due to their unique spectral response, while also helping to identify which markers or bands are the best for detecting differences between similar species and to facilitate a more rapid classification (Schmid et al. 2004).

The overarching objectives for this study were to determine if and to what extent remote sensing may be useful for monitoring wetland vegetation (species and types) with an eye towards the evaluation of mitigation success. Our end-goal was to create a spectral library and model for wetlands in Western New York State and to evaluate the use of individual bands to identify characteristic types of vegetation. To this end, we selected created and natural wetland sites in western New York State and collected canopy-level and laboratory spectral measurements of *Phragmites australis* (Common reed) (PHRAG), *Thypha latifolia (*Broadleaf cattail) (BLC), *Typha angustifolia* (Narrowleaf cattail) (NLC), and *Phalaris arundinacea* (Reed canarygrass) (RCG), the four common invasive wetland plants in this region. Our specific questions were:

1.) ***Are we able to differentiate between visually similar species using their spectral signatures?***

2.) ***Are wavelengths that are determined to be useful for identifying species on a field canopy-level also useful for identifying the same species in an aerial image?***

3.) ***Can we suggest specific wavelengths or spectral regions for a multi-spectral sensor that could produce similar results and be more readily available and cost effective for land managers to use in the future?***

## MATERIALS AND METHODS

*Site Description:*

Four wetlands, two natural (N1 and N2) or reference wetlands and two constructed wetlands (C1 and C2), on the Rochester Institute of Technology (RIT) campus in Rochester, New York (43$^{O}$4'59.82"N, 77$^{O}$40'32.10"W) were selected for this study (Figure 1 and Appendix II). These four emergent wetlands contain similar vegetation communities, are fed by groundwater, and are part of the Red Creek watershed, within the larger Genesee River watershed (Scheiner 2011).

Natural Wetland 1 (N1) is located on the southern part of the campus (about 1.2 ha); the northern edge of the wetland is bordered by wooded wetlands that act as a buffer between the wetland and an apartment complex, and the southern edge slopes toward an upland meadow. Natural Wetland 2 (N2), (1 ha) is located on the north end of the campus with herbaceous plant species along the edges. Red Creek runs along the northern edge of the wetland and a drainage ditch is present in the wetland on the eastern side that loops around the north into Red Creek.

In 2002, USACE required RIT to build a compository wetland complex what is now referred to as Constructed Wetland 2 (C2). The total size of C2 is 5.6 ha which includes ponds, wet meadows and forested wetlands and buffer zones, but the study site was limited to 1 ha of the site where the wet meadow and emergent habitats are located. C2 is located to the north of C1 and east of the utility yard (Figure 1). The predominant areas consist of open water with small areas of grassy meadows surrounding it, a small woody area, and persistent emergent plants are along the edges of the open water.

In 2007, the northeast section of the RIT campus was sold to Wilmorite Properties, for the development of the Park Point complex at RIT. This tract of land was previously classified as state and federal forested and emergent wetlands. As part of the permit that was obtained by Wilmorite from the DEC and the USACE, Constructed Wetland 1 (C1) was created on the southeastern section of the RIT campus, and consists of a mix of meadow, open water, persistent emergent, and herbaceous emergent plant communities. The C1 study site is only a small portion of the total wetland (1 ha of 29 ha), because additional planting efforts were underway in other sections of the mitigation area (Scheiner 2011).

Perimeters of each wetland complex, the center point of large vegetation monocultures, and permanent vegetation monitoring plots were mapped using a Trimble Geographic Positioning System (GPS) Unit with sub-meter accuracy. The permanent vegetation plots were established in the summer of 2009 by surveying vegetation in each wetland using a 10 x 10 m grid to establish the dominant vegetation types in 1 $m^2$ plots at the grid intersections (Scheiner 2011). Within each wetland three plots of each community type were chosen at random to serve as permanent sampling plots, with the number of permanent plots per wetland determined by the number of distinct vegetative communities. Seasonally, from 2009 forward (spring, summer, fall), vegetation surveys have taken place and the percent cover of all individual species has been recorded for each plot.

*Field and Laboratory Data Collection:*

In July 2010, the company SpecTIR (www.spectir.com) conducted a flyover of the RIT campus between 10 am and 2 pm EST to collect hyperspectral imagery of the campus. At the

same time a large-scale ground-truthing effort was undertaken. At each permanent plot, vegetation samples were collected and three tiers of reflectance measurements were made at canopy-level (1 $m^2$), leaf-level, and in the laboratory.

Canopy-level reflectance (n>3) was measured using an Ocean Optics Red Tide spectrometer with a reflectance probe suspended 1.5 m above the canopy. Prior to each measurement, a dark target reflective measurement was taken by covering the sensor, and a white reference was used to calibrate the spectrometer based on a stable, diffuse reference panel with assumed 100% reflectivity in the 300-1000 nm range. Leaf-level measurements were made for each plant species (or bare ground) that comprised >20% of the total canopy cover, by grouping leaves together (n = 3 per species). Twelve leaves for each of these species were then collected, bagged and brought back to the laboratory where reflectance were once again measured by grouping leaves together in the controlled laboratory environment using Analytical Spectral Devices, Inc., Boulder, Colorado, ViewSpec software (ASD).

*Processing and Analysis of Field and Lab Spectra:*

Both field and laboratory spectra were smoothed in Microsoft Excel using weighted five-wavelength averaging to minimize sensor and atmospheric noise. Samples or specific wavelengths with negative or invalid values were removed from the dataset and the first and second derivatives were calculated (Equations I and II). Average reflectance values were calculated for each species of interest and plotted to visually evaluate differences among species. The available wavelengths were then compared across all three data sets, and the range of wavelengths was limited to those mutually available. The resulting range of wavelengths that

were used for further analysis were 446, 447, 453-892 nm for reflectance, 446, 447, 453-891 nm for the first-derivatives and 446, 447, 453-890 nm for the second-derivatives.

Linear discriminant analysis functions were calculated for each of the datasets using SAS v9.1 Software (SAS Institute Inc., Cary, NC). Each dataset was analyzed separately (canopy-, leaf-, and laboratory-level), using all values (reflectance, first-, and second-derivatives), and also using only the original reflectance values. The latter approach facilitates comparison with the aerial imagery and aids in identification of important wavelengths or regions on the electromagnetic spectrum for a multi-spectral sensor. We used $\alpha < 0.1$ for the discriminant analysis so that the resulting output contained no more than 15 wavelengths that were deemed to be useful for species classification (see Appendix III for sample script). This resulted in a list of important wavelengths for differentiating between species that were inserted into a SAS script with a set of weighted algorithms that can be used for species identification. Linear discriminant functions were subsequently used in SAS on specific datasets to assess accuracy using a leave-one-out cross-validation approach (Equations III – VI). Cross-validation confusion matrices were created for all analysis to calculate the accuracy rating for producer, user, overall and Kappa (Congalton 1991).

For the purpose of this study the linear discriminant functions derived from the canopy-level dataset only were used for further analysis, because we wanted to determine the legitimacy of using these models for our ultimate goal of species identification on a large-scale using imagery.

*Imagery Collection and Analysis:*

Hyperspectral imagery of the landscape was collected during the flyovers along specific flight paths. Data were captured in the 350-2000 nm range across 360 bands, with a spatial resolution of 1 $m^2$. The flyover included four flight paths of the RIT campus, each of which was 300 m wide. Two of these were flown north and south, one was flown northwest to southeast, and the final one was flown east-west (Herweg et al. 2012). Two separate flight paths captured the four wetlands of interest (one contained N1, and the second N2, C1 and C2). The hyperspectral imagery was ortho-rectified and pre-processed to reflectance using Environment for Visualizing Images (ENVI v4.7) software (ENVI 2004).

Regions of interest (ROIs) were created in ENVI using the wetland perimeters that were collected using a handheld Trimble unit with an accuracy of 1 $m^2$. The ROIs were overlain on the images and the image file was subset based on the perimeters so that the resulting image file only included the pertinent wetlands, reducing processing time and eliminating extraneous features, such as buildings, cars, and roads that may add to the spectral variance within the image. Then the two new image files containing only the wetlands were mosaicked together to form a single image file with all four wetlands that facilitates comparison among wetlands. We have assumed that the differences between flights were negligible because the flights were conducted on the same day with the same atmospheric conditions, by the same pilot, and were post-processed the same way.

Using the BandMath function in ENVI, we classified the image based on the canopy-level linear discriminant functions generated from the RIT 2010 canopy-level dataset for reflectance values only created a color-coded map to identify target locations for investigation by land managers. We matched the identified wavelengths (from the linear discriminant function

analysis) with the associated bands in the image using the header file (bands in the image were classified as band 1 – band 360 with each band representing a range of wavelengths between 350-2500 nm) (Equations VII – X). We were able to do this because even though the canopy data were based on 350-1000 nm sensor data, we were isolating specific wavelengths within the imagery, thus ignoring all of the other wavelengths that were not previously evaluated. This resulted in four separate image files in ENVI corresponding to each of the four species that were converted to *.img files and imported into ArcGIS Map v9.0 (ESRI, Redlands, CA) for further classification. Each species file was reclassified to exclude any negative values and then the histograms were viewed to reclass the pixels to Boolean values. The reclassed image files were overlaid using a weighted sum to produce a classification map that identifies each pixel based on the canopy-level model. The resulting classification map was overlaid with ground-truth GPS points that were collected during the vegetation surveys and while collecting the field spectra to assess per-species producer accuracy (within a 3 m radius/buffer).

In addition, an unsupervised classification was also run on the mosaicked image file containing all four wetlands to evaluate differences between a model-based classification and an ENVI endmember classification. In ENVI the image file was opened and using the Spectral Hourglass Wizard function a Minimum Noise Fraction (MNF) and Spectral Angle Mapper (SAM) analysis were run. For the MNF analysis the spatial coherence threshold was set to 0.72, resulting in 11 bands above the threshold. The resulting SAM classification was then exported to ArcGIS for further identification of the 11 different classes. Identification of the classes was done by the producer using aerial images of the wetlands, vegetation surveys, and ground control points.

## RESULTS AND DISCUSSION

The purpose of this study was to determine the usefulness of using remote sensing approaches for monitoring wetland vegetation for use in mitigation assessment. We selected created and natural wetland sites in Western New York State (located on the RIT campus) and collected canopy-level, laboratory-level, and aerial spectral measurements of four common wetland plants, *Phragmites australis* (Common reed) (PHRAG), *Thypha latifolia (*Broadleaf cattail) (BLC), *Typha angustifolia* (Narrowleaf cattail) (NLC)*,* and *Phalaris arundinacea* (Reed canarygrass) (RCG), to determine if remote sensing is a viable method for wetland monitoring.

***Are we able to differentiate between visually similar species using their spectral signatures?***

The first step was to determine if our species of interest were spectrally separable, and if so, determine the wavelength regions that are useful for species differentiation. The canopy-level reflectance curves for each species followed the generic curvature expected for plants (Figure 2). RCG though, had a higher reflectance value, especially in the near-infrared region, than the other three species in both canopy, leaf-level and lab measurements (Figure 2, Figure 3, and Figure 4). We may attribute this difference to a distinct structure, including thinner stalks and leaves, smaller stature, and waxier leaves that may reflect more light. In the visible spectrum, the two visually similar congeneric cattail species (NLC and BLC) were distinct, but along the red-edge and in the near infrared region the reflectance values for NLC were higher, perhaps due to the thinner leaves of NLC (Figure 2). The leaf-level spectra for these two species show a similar distinction (Figure 3) suggesting wavelengths within these regions may be useful for field differentiation. The difference between the laboratory and canopy and leaf-level spectra for the cattails (Figures 2, 3 and 4) may be attributed to the difference in canopy structure and presence

of distinct inflorescences that are missing during the lab measurements. These results suggest that not only leaf structure but also the inflorescences influence the spectral reflectance.

From the discriminant analysis we were able to identify specific wavelengths that were useful for discriminating among the four species of interest. While similar regions within the visible electromagnetic spectrum were useful for all datasets, and all included blue (380-495 nm), red (590-679 nm), red-edge (680-799 nm) and near-infrared (800-1300 nm) regions (Table 1), the specific wavelengths varied among the different tiers of data. The field samples relied more heavily on the red-edge and near-infrared regions than the leaf- or lab-datasets, while the leaf-level results were more strongly weighted towards the green region. These differences are most likely due to the way the samples were collected. The lab-level data were collected from flattened leaves only, resulting in differences associated primarily with pigments and coloring in the visible region. For the leaf-level samples, the spectral probe was held close to the leaves, thereby limiting atmospheric interaction in the blue region. This is in contrast to the canopy-level measurements that included atmospheric interactions along with the general structure of the plant, including leaves, stems and inflorescences, and likely represents the most useful and holistic view of the spectra.

Linear discriminant functions (Equations III through VI) were developed for the four species of interest using the canopy-level derived wavelengths deemed most important for species differentiation and the results were assessed using a classification cross-validation matrix for the four wetlands on the RIT campus (Table 2). The field canopy-level dataset yielded a relatively high accuracy for all wetlands. Using the combined reflectance, first derivatives, and second derivatives we found that BLC and NLC were classified correctly, with an accuracy of 66.67% and 81.25%, respectively, while PHRAG and RCG both had an accuracy of 100%

(Table 2). However, using reflectance alone (without the first- and second-derivatives), the accuracy ratings were substantially higher for BLC and NLC (92.86% and 90.00%, respectively) (Table 3). This is counter to prior studies that found greater species differentiation using first-derivatives (van Aardt and Wynne 2001). The ability to differentiate between the congeneric and structurally similar BLC (native) and NLC (non-native) is valuable and promising, and suggests that there are subtle differences picked up by the spectral analysis. We used a Kappa error matrix to determine if the model provides values that are significantly better than random sampling (Congalton 1991; Jensen 1996). The Kappa value for the reflectance only model (0.92) was higher than for the full model (0.77), again suggesting the greater power of the reflectance only model and validating that we can successfully differentiate among these four plant species. Our high accuracy ratings and the results of the Kappa analysis validate that using a step-wise discriminant analysis we successfully identified and separated four major wetland invasive species, with accuracy rating considered acceptable within the remote sensing field (van Aardt and Wynne 2001). Given the successful differentiation using field spectra, the next step was to determine if we can use a similar approach with aerial imagery, thus providing a more powerful tool for managers to rapidly evaluate species composition of large swaths of land.

Although created wetlands are supposed to be modeled after natural wetlands there is still a possibility for differences fundamentally within the same species spectra. Figure 5 displays the canopy-level data for NLC samples that were collected at the natural and created wetlands on the RIT campus. The natural wetland samples have higher reflectance values along the red-edge and the near-infrared regions. This could be due to a structural difference in the plants since the created wetlands are newer than the natural wetlands, or a difference in nutrient availability, such as nitrogen, or a hydrological and soil difference in the wetland itself. Further research would

need to be done to determine if there are large differences between natural and created wetlands, and if so this would result in a need for two separate models for wetland vegetation classifications.

Now, that we have been able to determine that we are able to differentiate between these four species using spectra collected out in the field, the next step would be to determine if we can also differentiate between these species using imagery.

***Are wavelengths that are determined to be useful for identifying species on a field canopy level also useful for identifying the same species in an aerial image?***

Comparison with the aerial imagery will allow us to determine if this imagery and associated wavelengths can be reliably used to characterize wetland invasive species on a large scale, saving valuable field monitoring time. The results of the model based classification were variable. Figures 6, 7 and 8 show the classification results for the created and the natural wetlands. It is important to note that because the model is only based on the four species, everything within the image was classified as either one or a combination of these species, including open water, shallow water, bare ground, and trees and shrubs. In all three figures a large portion of the area was classified as BLC; though some pixels are correct, such as the two patches in the southern section of the wetland (Figure 6), others are not. Natural Wetland 2 (Figure 8) was mostly classified as BLC even though it is predominantly made up of NLC. It is also important to note that the model did not display any PHRAG patches in the created wetlands (Figure 6) or in Natural Wetland 1 (Figure 7), in spite of its clear presence at these sites. Thus, even though we achieved a high accuracy rating for the canopy-level data, it does not correlate well with the aerial-level data. The classifications are also poorly correlated with the ground control points that were collected (Figure 9), particularly for PHRAG Created Wetland 1. None

of these GPS points were near pixels that would be classified as PHRAG, instead classifying the majority of them as RCG and BLC. Although beyond the scope of this study, improvements to aid in better classification of aerial imagery include 1.) collecting more samples of the various species from the field in different types of environments, such as monocultures in dry areas and wet areas; 2.) including data collected for bare ground, common trees and shrubs found in the area; and 3.) clipping out sections of open water from the original aerial image before running the analysis.

An unsupervised Spectral Angle Mapper (SAM) classification was run on the original image to determine if the reason why the aerial image canopy-level model classification was not very accurate because of the types of plant communities present or because of the actual model used. The resulting classification maps for the RIT wetlands (Figures 10, 11, and 12) show that because of the large variance in vegetation types and abiotic structures within the image we may only be able to delineate generic community types with a 0.72 spatial coherence threshold. The resulting images may be useful in mapping out specific types of vegetation and generic areas, but are not useful for individual species classification. A few adjustments to improve this outcome may include 1.) eliminating large open water pixels from the image before running the unsupervised classification; 2.) lowering the threshold to increase the number of classes (note that this will require either a very well defined aerial image or a larger number of ground control points); and 3.) run a supervised classification on the image using ground control points to identify pixels and endmembers that are specific to the species that we are interested in.

***Can we suggest specific wavelengths or spectral regions for a multi-spectral sensor that could produce similar results and be more readily available and cost effective for land managers to use in the future?***

Ideally, the end goal of this research is to create a multi-spectral sensor capable of collecting wavelengths appropriate for wetland plant delineation. We identified specific regions within the electromagnetic spectrum that were useful for differentiating among these four plant species of interest. Promising bands were contained within the blue (446 nm), red (670 nm) red-edge (686 nm, 690 nm and 711 nm) and near-infrared (849 nm, and 888 nm) regions (Table 4). We note, however, that results are based on four ecologically similar sites and that additional studies in this region are required to increase the sample size and to determine site-specifically of the model.

## CONCLUSION

In conclusion, we were able to reliably discriminate among four wetland invasive species for the wetlands on the Rochester Institute of Technology campus using canopy-level data. We found that when classifying PHRAG and RCG were not misclassified or confused with the *Typha* species, and that the raw reflectance values were more useful for classifying between both species of *Typha*. We also noted that when looking at the spectral signatures of each of the species, RCG had higher reflectance values then the other three species, and along the red-edge and near-infrared region NLC tended to have higher reflectance readings than BLC. Though, it is important to note that all of these results are based on four study sites, collected on a single date, leading to limited application beyond the immediate region and time of year without further comparative studies. The next steps are to increase the sample size both temporally and spatially by sampling in multiple years and at different sites.

In addition further work would also need to be done to see if there are differences between natural and created wetlands on a species level. As we saw for NLC, there are subtle differences in the reflectance values for plants found in created versus natural wetlands. If there are consistently different curvatures for the same species found in different wetlands then different models would need to be established for classification purposes for both natural and created wetlands. It is important to look into this topic because if there are subtle differences in species reflectance values and spectra based on if they are found in a natural versus a created wetland this can impact the results and the accuracy of the model and a different technique would need to be used by land managers to classify natural versus created wetlands.

When the canopy-level data model was extrapolated to aerial imagery it did not have as high of a success rating. Further work needs to be done on this model to be able to utilize it on an

imagery level, such as including an equation for trees and shrubs, and eliminating open water from the image before classifying, as well as increasing the sample size from the canopy-level model to make a more robust equation. It is still too early to say that the model will not work, this is just the first trial of this type of method and more adjustments and studies need to be done.

The overall purpose of the study was to identify techniques and models that could help land managers when performing vegetation mapping and to reduce the time needed for doing vegetation monitoring prior to actual remediation. This is a good first step at investigating the possible usage of remote sensing techniques for wetland field monitoring but more research is needed to determine if a generic model is versatile enough to be used in all of western New York.

## TABLES AND FIGURES

**Table 1.**
Resulting wavelengths from the discriminant analysis for each tier. This chart represents the analysis done when limiting the sample size to only the initial reflectance values from 350 nm – 1000 nm (excluding the first- and second-derivatives). The table is in order, from top to bottom, with the top number being the most useful in discriminating between species. These were the wavelengths that were then used to create the linear discriminant functions.

| **Important wavelengths per tier of data for RIT Wetlands** | | | |
|---|---|---|---|
| Discriminant Of… | Reflectance Values (raw data) Canopy-level (4 classes) (53 samples) | Reflectance Values (raw data) Leaf-level (4 classes) (53 samples) | Reflectance Values (raw data) Lab Data (4 classes) (41 samples) |
| α level | 0.01 | 0.1 | 0.05 |
| Wavelength (nm) | 888 | 540 | 447 |
| | 849 | 556 | 455 |
| | 446 | 534 | 462 |
| | 690 | 547 | 461 |
| | 670 | | 468 |
| | 711 | | 465 |
| | 686 | | 480 |
| | | | 477 |
| | | | 481 |

**Table 2.**

Cross-validation confusion matrix of the canopy-level field samples that were taken using the reflectance, first- and second-derivative values.

| **RIT 2010 Canopy-level Cross Validation Matrix (Reflectance, 1st Derivative and 2nd Derivative Values All Together)** | | | | | | |
|---|---|---|---|---|---|---|
| | **Reference Data** | | | | | **User Accuracy (%)** |
| | BLC | NLC | PHRAG | RCG | **Totals** | |
| BLC | 12 | 3 | 0 | 0 | **15** | **80.00** |
| NLC | 6 | 13 | 0 | 0 | **19** | **68.42** |
| PHRAG | 0 | 0 | 9 | 0 | **9** | **100.00** |
| RCG | 0 | 0 | 0 | 10 | **10** | **100.00** |
| **Totals** | **18** | **16** | **9** | **10** | **53** | **87.11** |
| **Producer Accuracy (%)** | **66.67** | **81.25** | **100.00** | **100.00** | **86.98** | 87.11 |
| Overall Accuracy (%) | | 83.02 | | | | |
| Kappa Accuracy | | 0.77 | | | | |

**Table 3.**

Cross-validation confusion matrix of the canopy-level for reflectance values only.

| **RIT 2010 Canopy-level Cross Validation Matrix (Reflectance Values Only)** | | | | | | |
|---|---|---|---|---|---|---|
| | **Reference Data** | | | | | **User Accuracy (%)** |
| | BLC | NLC | PHRAG | RCG | **Totals** | |
| BLC | 13 | 2 | 0 | 0 | **15** | **86.67** |
| NLC | 1 | 18 | 0 | 0 | **19** | **94.74** |
| PHRAG | 0 | 0 | 9 | 0 | **9** | **100.00** |
| RCG | 0 | 0 | 0 | 10 | **10** | **100.00** |
| **Totals** | **14** | **20** | **9** | **10** | **53** | **95.35** |
| **Producer Accuracy (%)** | **92.86** | **90.00** | **100.00** | **100.00** | **95.71** | 95.35 |
| Overall Accuracy (%) | | 94.34 | | | | |
| Kappa Accuracy | | 0.92 | | | | |

**Table 4.**

Recommendations of regions within the electromagnetic spectrum and their corresponding bands that may prove useful when creating a multi-spectral sensor that would be more commercially viable based on the canopy-level field samples.

| **Canopy Level Analysis (Reflectance Only for Recommendations for Sensor)** | | |
|---|---|---|
| | **Visible Electromagnetic Spectrum** | RIT 2010 (53 samples) (4 classes) |
| α level | ---------- | 0.01 |
| Wavelength (nm) | Blue 380-495 | 446 |
| | Green 495-590 | |
| | Red 590-679 | 670 |
| | Red Edge 680-799 | 686 |
| | | 690 |
| | | 711 |
| | Near Infrared 800-1300 | 849 |
| | | 888 |

Small Importance Scale for Discriminant Functions High


**Figure 1.**
Rochester, NY (Monroe County) expanded to show Rochester Institute of Technology campus. Image of RIT campus displays the perimeters of the four wetlands of interest (going clockwise starting at the top of the image: N1, C2, C1, N2).

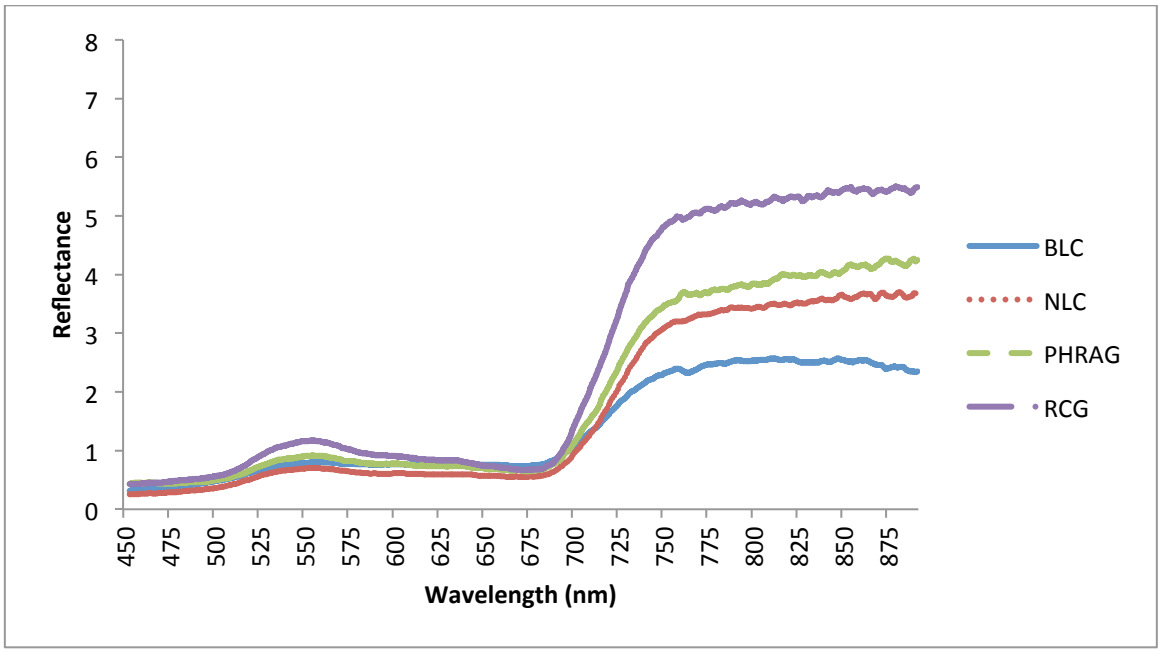


**Figure 2.**
Average spectra across wetlands for Broadleaf cattail (BLC), Narrowleaf cattail (NLC), Common reed (PHRAG) and Reedcanary grass (RCG) for the canopy-level dataset.

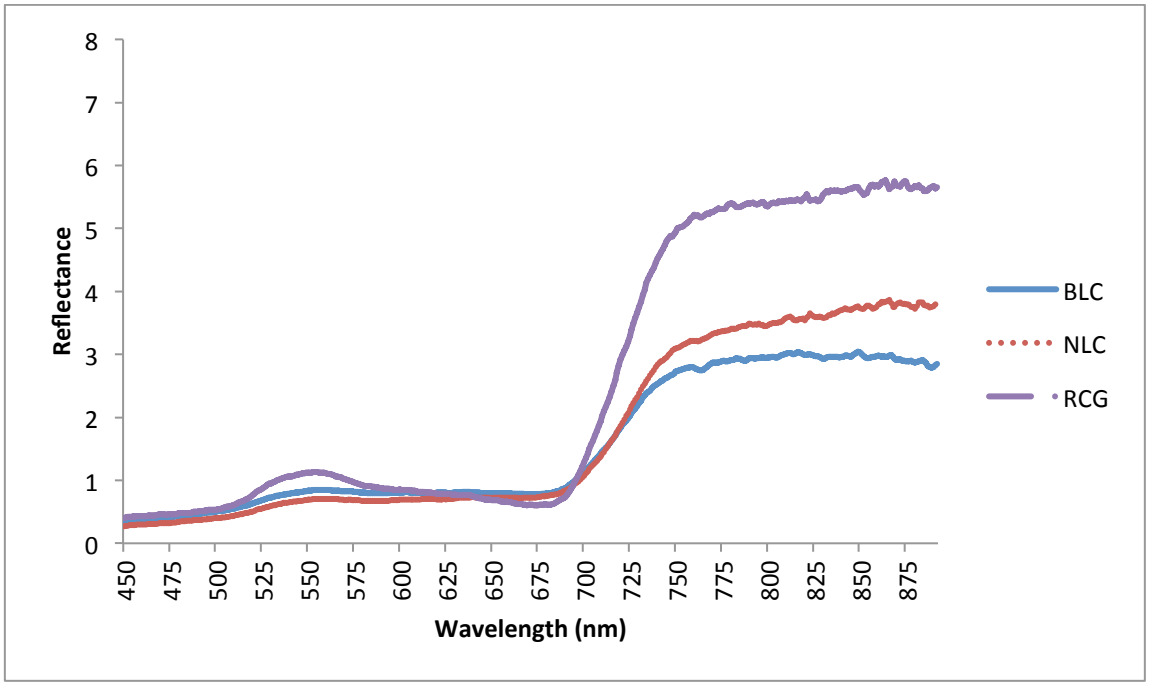


**Figure 3.**
Average leaf-level spectra per wavelength for each of the three species (PHRAG samples were removed from the subset due to invalid values during processing).

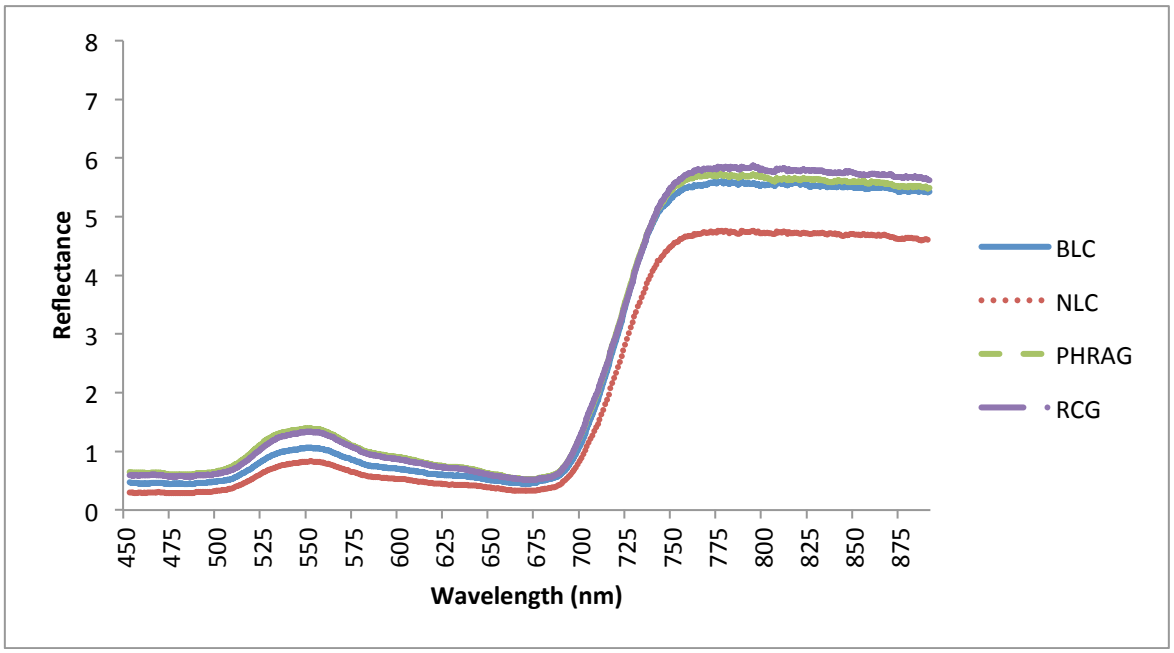


**Figure 4.**
Average laboratory-level spectra per wavelength for each of the four species.

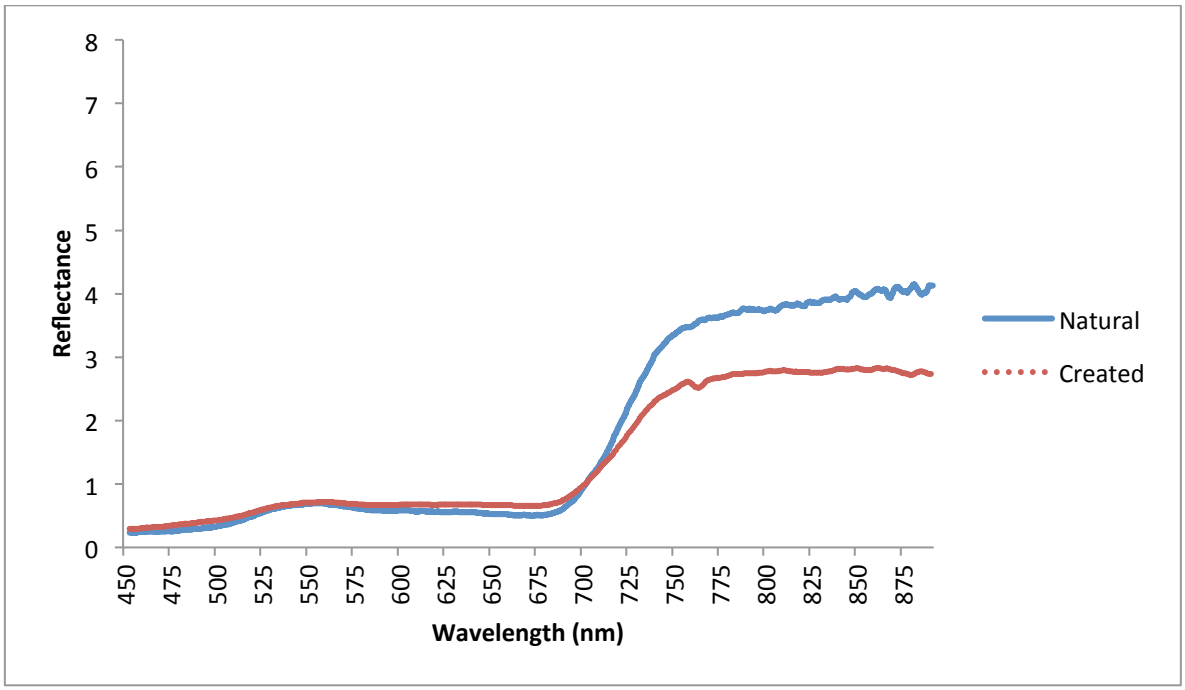


**Figure 5.**
NLC canopy-level samples found on the RIT campus for natural and created wetlands.

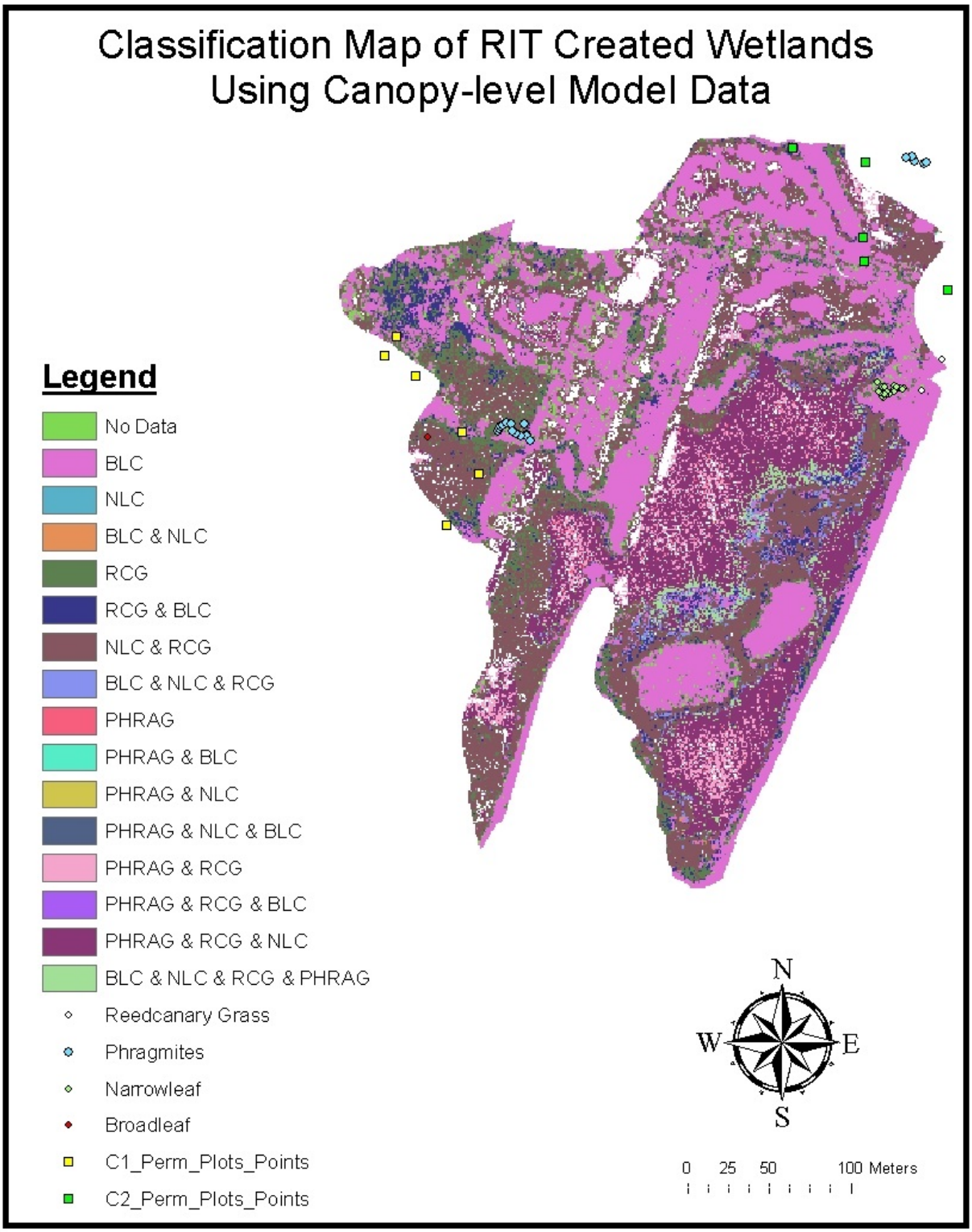


**Figure 6.**

Classification map of created wetlands (C1 and C2) on RIT campus based on the linear discriminant analysis functions that were developed from the canopy-level data with ground control points of some monoculture patches of the four invasive species.

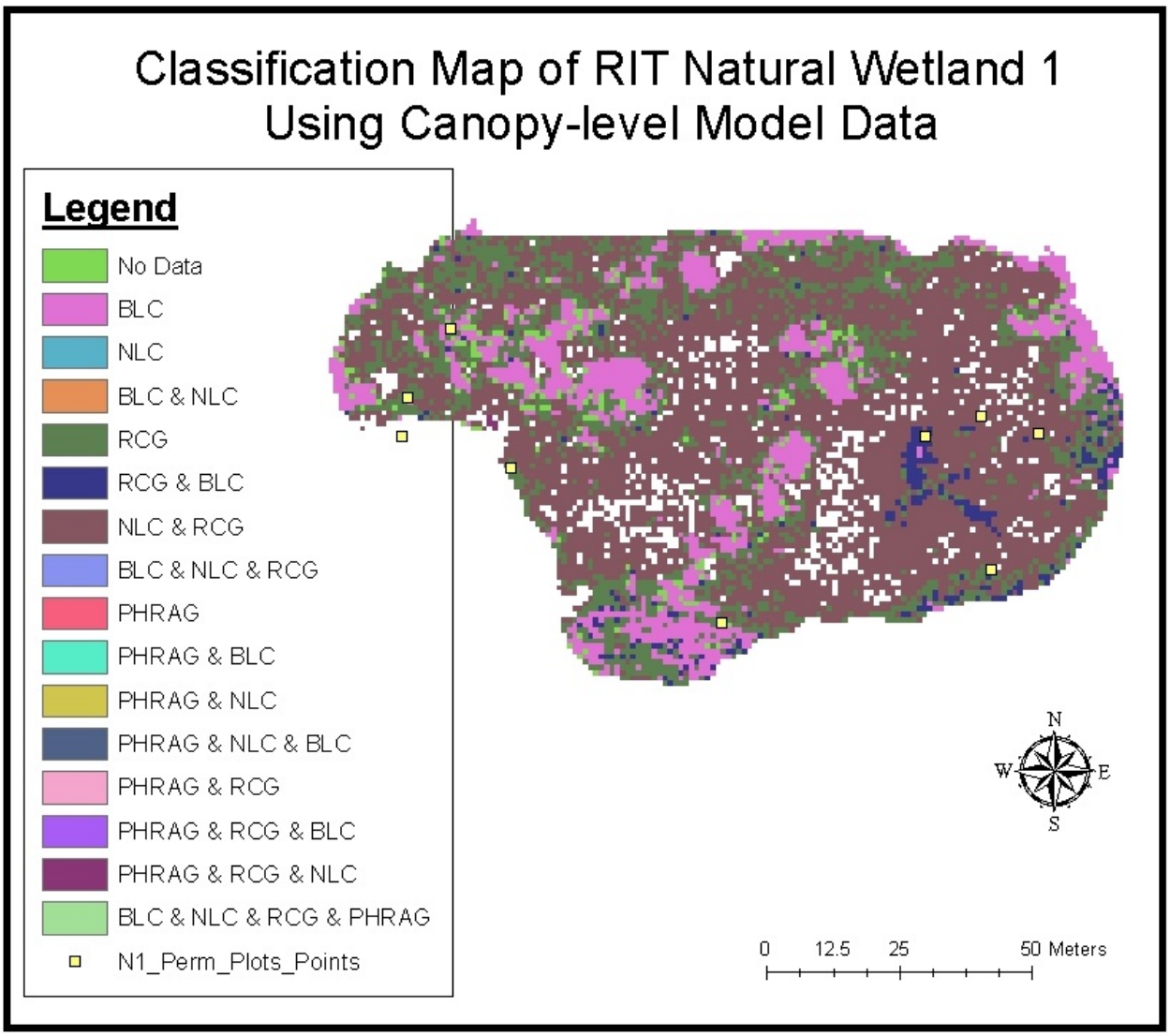


**Figure 7.**

Classification map of Natural Wetland 1 (southern wetland) on RIT data. campus based on the linear discriminant analysis functions that were developed from the canopy-level.

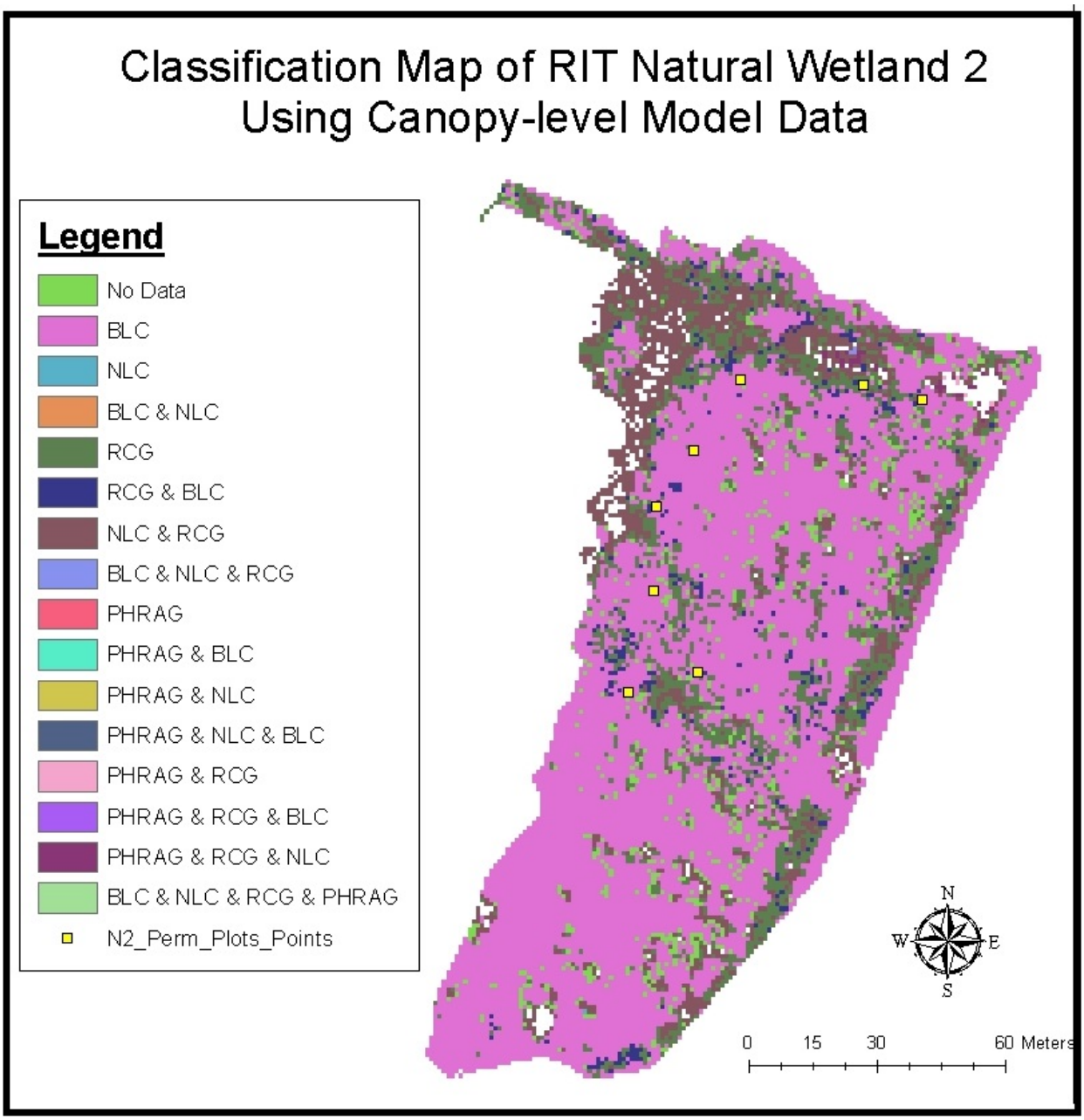


**Figure 8.**

Classification map of Natural Wetland 2 (northern wetland) on RIT campus based on the linear discriminant analysis functions that were developed from the canopy-level data.

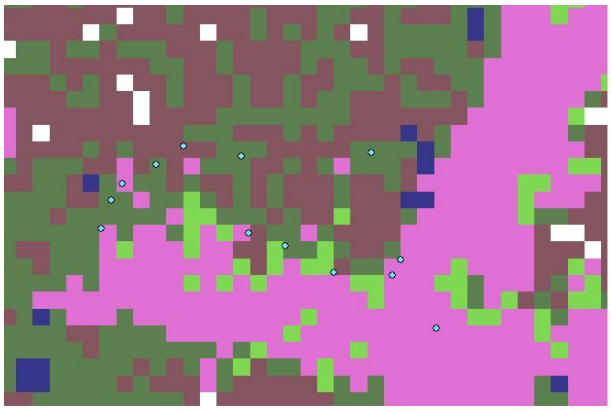

**Figure 9.**

Zoomed in image of the Classification Map for RIT Created Wetlands Using Canopy-level Model Data where the PHRAG ground control points were collected. The resulting image shows 13 PHRAG ground control points that were collected in a monoculture PHRAG patch. The results show that none of the points are near pixels that would be classified as PHRAG, and a majority of them are located where the map is classifying RCG and BLC should be found.

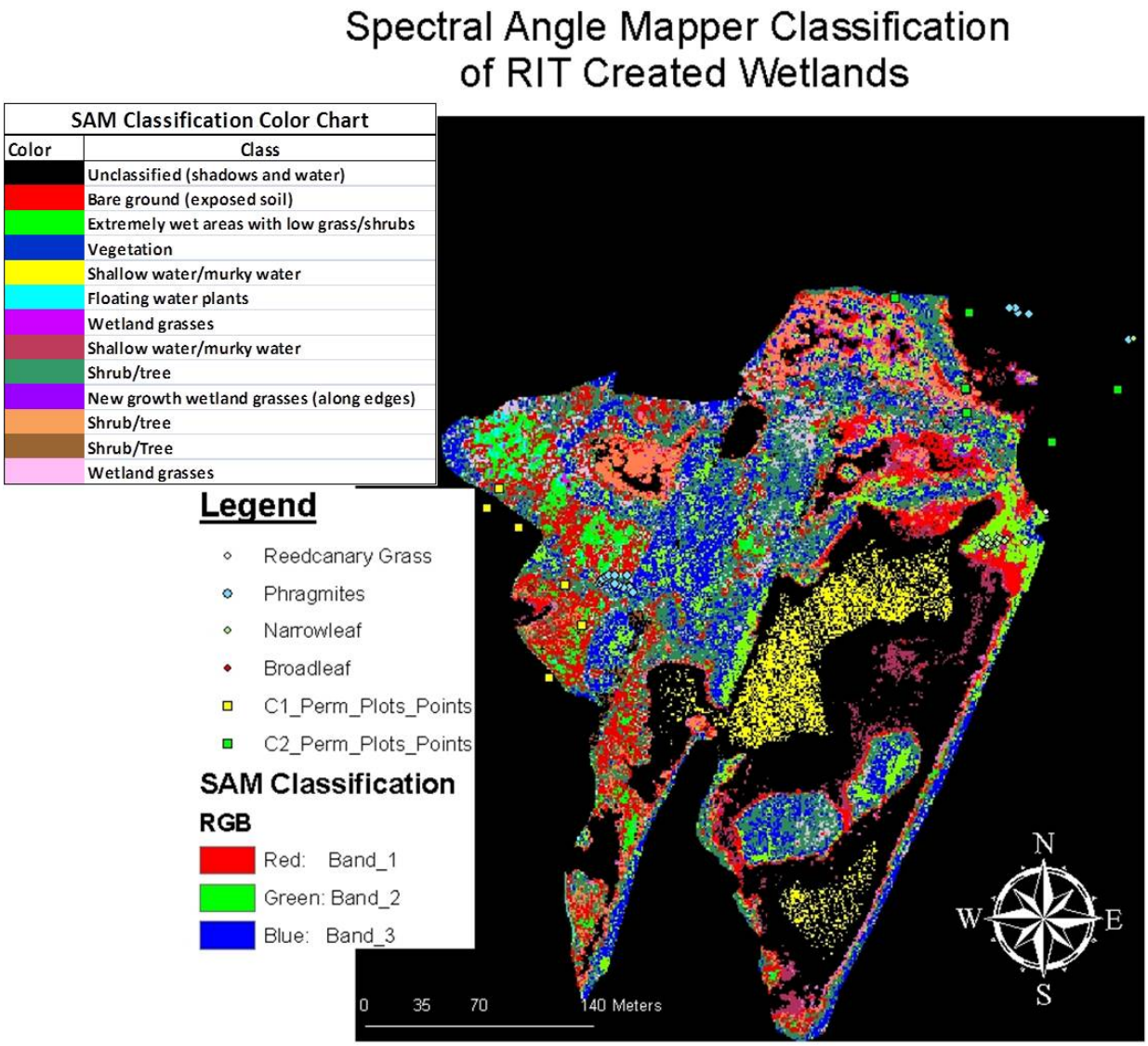


**Figure 10.**

Unsupervised Spectral Angle Mapper (SAM) Classification of aerial image for RIT created wetlands (C1 and C2). Classification was not able to go down to the species level.

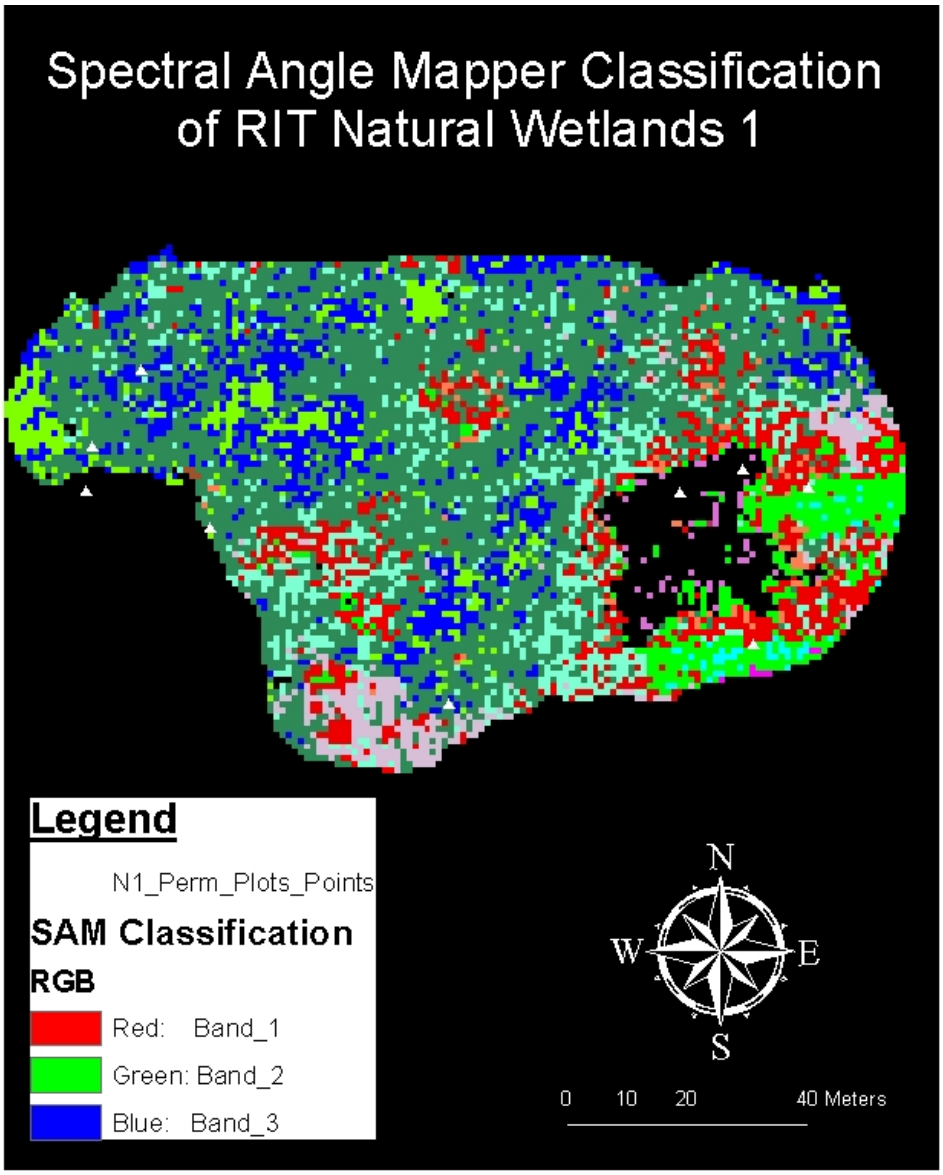


**Figure 11.**

Unsupervised Spectral Angle Mapper (SAM) Classification of aerial image for RIT Natural Wetland 1. Classification is not able to go down to the species level.

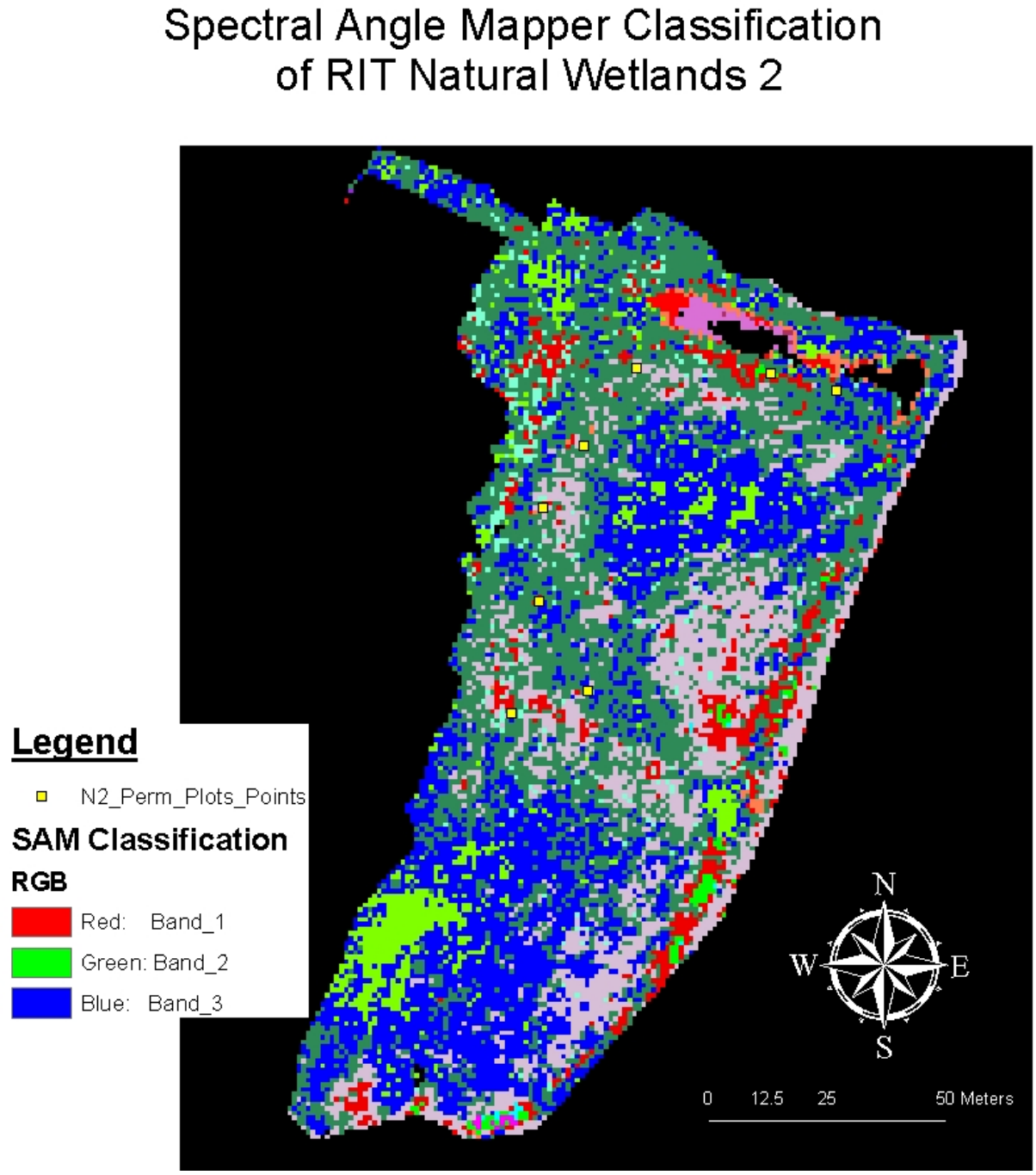


**Figure 12.**

Unsupervised Spectral Angle Mapper (SAM) Classification of aerial image for RIT Natural Wetland 2. Classification is not able to go down to the species level.

**Equation I: Reflectance 1st Derivative**

$$\frac{\Delta y}{\Delta x} = \frac{(\text{reflectance variable}_2 - \text{reflectance variable}_1)}{(\text{wavelength}_2 - \text{wavelength}_1)}$$

**Equation II: Reflectance 2nd Derivative**

$$\frac{\Delta y}{\Delta x} = \frac{(\text{Value of } 1^{st} \text{ Derivative}_2 - \text{Value of } 1^{st} \text{ Derivative}_1)}{(\text{wavelength}_2 - \text{wavelength}_1)}$$

**Equation III: Model for BLC**

BLC = -18.40105 – (41.63981 x 888 nm) + (42.04642 x 849 nm) + (10.86097 x 446 nm) – (7.97286 x 690 nm) + (11.04740 x 670 nm) + (18.02880 x 711 nm) – (2.15667 x 686 nm)

**Equation IV: Model for NLC**

NLC = -13.37609 – (24.50523 x 888 nm) + (27.71680 x 849 nm) – (17.12783 x 446 nm) + (2.74544 x 690 nm) – (4.12695 x 670 nm) + (9.81065 x 711 nm) + (9.37594 x 686 nm)

**Equation V: Model for PHRAG**

PHRAG = -21.82961 – (1.37320 x 888 nm) + (27.71680 x 849 nm) – (17.12783 x 446 nm) + (2.74544 x 690 nm) – (4.12695 x 670 nm) + (9.81065 x 711 nm) + (9.37594 x 686 nm)

**Equation VI: Model for RCG**

RCG = -40.41372 – (57.74955 x 888 nm) + (54.21557 x 849 nm) + (65.15441 x 446 nm) – (201.94196 x 690 nm) + (108.15327 x 670 nm) + (64.71868 x 711 nm) + (36.01220 x 686 nm)

**Equation VII: Imagery Equation for BLC**

BLC = -18.40105 – (41.63981 x Band 107) + (42.04642 x Band 99) + (10.86097 x Band 12) – (7.97286 x Band 65) + (11.04740 x Band 61) + (18.02880 x Band 70) – (2.15667 x Band 64)

**Equation VIII: Imagery Equation for NLC**

NLC = -13.37609 – (24.50523 x Band 107) + (27.71680 x Band 99) – (17.12783 x Band 12) + (2.74544 x Band 65) – (4.12695 x Band 61) + (9.81065 x Band 70) + (9.37594 x Band 64)

**Equation IX: Imagery Equation for PHRAG**

PHRAG = -21.82961 – (1.37320 x Band 107) + (27.71680 x Band 99) – (17.12783 x Band 12) + (2.74544 x Band 65) – (4.12695 x Band 61) + (9.81065 x Band 70) + (9.37594 x Band 64)

**Equation X: Imagery Equation for RCG**

RCG = -40.41372 – (57.74955 x Band 107) + (54.21557 x Band 99) + (65.15441 x Band 12) – (201.94196 x Band 65) + (108.15327 x Band 61) + (64.71868 x Band 70) + (36.01220 x Band 64)

## REFERENCES


Adam, Elhadi, Onisimo Mutanga, and Denis Rugege. 2009. "Multispectral and Hyperspectral Remote Sensing for Identification and Mapping of Wetland Vegetation: a Review." *Wetlands Ecology and Management* 18 (3) (December 11): 281–296.

Artigas, Francisco J, and Jiansheng Yang. 2006. "Spectral Discrimination of Marsh Vegetation Types in the New Jersey Meadowlands, USA." *Environmental Research* 26 (1): 271–277.

Balcombe, Collin K, James T Anderson, Ronald H Fortney, James S Rentch, William N Grafton, Walter S Kordek, and West Virginia. 2005. "A Comparison of Plant Communities in Mitigation and Reference Wetlands in the mid-Appalachians." *Wetlands* 25 (1): 130–142.

Barona, Moises Y, Richard B Gomez, and William Roper. 2003. "Hyperspectral Applications in Wetland Characterization." In *SPIE Vol. 5097: Geo-spatial and Temporal Image and Data Exploitation III*, 5097:197–206.

Becker, Brian L., David P. Lusch, and Jiaguo Qi. 2005. "Identifying Optimal Spectral Bands from in Situ Measurements of Great Lakes Coastal Wetlands Using Second-derivative Analysis." *Remote Sensing of Environment* 97 (2) (July): 238–248.

Brinson, Mark M, and Richard Rheinhardt. 1996. "The Role of Refernce Wetlands in Functional Assessment and Mitigation." *Ecological Applications* 6 (1): 69–76.

Cho, Moses a., Pravesh Debba, Renaud Mathieu, Jan van Aardt, Greg Asner, Laven Naidoo, Russell Main, Abel Ramoelo, and Bongani Majeke. 2009. "Spectral Variability Within Species and Its Effects on Savanna Tree Species Discrimination." In *2009 IEEE International Geoscience and Remote Sensing Symposium*, II–190–II–193. Ieee.

Clean Water Act. 1972. *Clean Water Act; Section 404*. Clean Water Act.

Congalton, Russell G. 1991. "A Review of Assessing the Accuracy of Classifications of Remotely Sensed Data." *Remote Sensing and Geospatial Technologies for Coastal Ecosystem Assessment and Management* 37: 35–46.

Dahl, Thomas E. 1986. *Wetlands Losses in the United States, 1780s - 1980s*. Washington, D.C.: U.S. Dept.of the Interior, Fish and Wildlife Service.

———. 1990. *Status and Trends of Wetlands in the Conterminous United States 1986 to 1997*. Washington, D.C.: U.S. Dept.of the Interior, Fish and Wildlife Service.

ENVI. 2004. "ENVI User's Guide". Research Systems, Inc.

Hall, Carlton R. 2004. “Plant Pigment Types, Distributions, and Influences on Shallow Water Submerged Aquatic Vegetation Mapping.” *Proceedings of SPIE* 5569: 183–193. doi:10.1117/12.565765.

Haslam, S.M. 2003. *Understanding Wetlands; Fen, Bog and Marsh*. London: Taylor & Francis Group.

Herweg, Jared a., John P. Kerekes, Oliver Weatherbee, David Messinger, Jan van Aardt, Emmett Ientilucci, Zoran Ninkov, et al. 2012. “SpecTIR Hyperspectral Airborne Rochester Experiment Data Collection Campaign.” In *SPIE Algorithims and Technologies for Multispectral, Hyperspectral and Unltraspetral Imagery XVIII*, edited by Sylvia S. Shen and Paul E. Lewis, 8390:839028–839028–10. Baltimore, MD, USA.

Huffman & Associates, Inc. 2000. “Wetlands Status and Trend Analysis of New York State Mid-1980s to Mid-1990s”. Vol. 2000. Larkspur.

Jensen, J.R. 1996. *Introductory Digital Image Processing: a Remote Sensing Perspective*. second edi. Upper Saddle River, New Jersey, USA: Prentice Hall Inc.

Jollineau, M. Y., and P. J. Howarth. 2008. “Mapping an Inland Wetland Complex Using Hyperspectral Imagery.” *International Journal of Remote Sensing* 29 (12) (June 15): 3609–3631.

Kent, Donald M. 2001. *Applied Wetlands Science and Technology*. 2nd ed. Boca Raton: Lewis Publishers.

Lacar, F M, M M Lewis, and I T Grierson. 2001. “Use of Hyperspectral Imagery for Mapping Grape Varieties in the Barossa Valley, South Australia.” *IEE* 0-7803-703 (C): 2875–2877.

Lyon, John G. 2001. *Wetland Landscape Characterization: GIS, Remote Sensing and Image Analysis*. Chelsea: Ann Arbor Press.

Manjunath, K. R., Shibendu Shankar Ray, and Sushma Panigrahy. 2011. “Discrimination of Spectrally-close Crops Using Ground-based Hyperspectral Data.” *Journal of the Indian Society of Remote Sensing* 39 (4) (June 3): 599–602.

National Research Council. 2001. “Compensating for Wetland Losses Under the Clean Water Act.”

“New York State Wetlands Assessment (Section 305(b)).” 2005. Albany.

Niagara Frontier Wildlife Habitat Council. 2013. “Wetlands.” *Western New York Land Conservancy Land Conservancy*. http://www.nfwhc.org/wetlands1.htm.

Rosso, P. H., S. L. Ustin, and A. Hastings. 2005. “Mapping Marshland Vegetation of San Francisco Bay, California, Using Hyperspectral Data.” *International Journal of Remote Sensing* 26 (23) (December 10): 5169–5191.

Scheiner, Katrina R. 2011. “Comparison of Geochemical and Biological Characteristics of Natural and Constructed Wetlands in Western NY”. Rochester Institute of Technology.

Schmid, T., M. Koch, J. Gumuzzio, and P. M. Mather. 2004. “A Spectral Library for a Semi-arid Wetland and Its Application to Studies of Wetland Degradation Using Hyperspectral and Multispectral Data.” *International Journal of Remote Sensing* 25 (13) (July): 2485–2496.

Schmidt, K.S., and A.K. Skidmore. 2003. “Spectral Discrimination of Vegetation Types in a Coastal Wetland.” *Remote Sensing of Environment* 85 (1) (April): 92–108.

Shippert, Peg. 2004. “Why Use Hyperspectral Imagery?” *Photogrammetric Engineering & Remote Sensing* (April): 377–379.

Siciliano, Daria, Kerstin Wasson, Donald C. DC Potts, and RC R.C. Olsen. 2008. “Evaluating Hyperspectral Imaging of Wetland Vegetation as a Tool for Detecting Estuarine Nutrient Enrichment.” *Remote Sensing of Environment* 112 (11) (November): 4020–4033.

Thenkabail, PS, BS Smith, and De Pauwe. 2002. “Evaluation of Narrowband and Broadband Vegetation Indices for Determining Optimal Hyperspectral Wavebands for Agricultural Crop Characterization.” *Photogrammetric Engineering and Remote Sensing* 68 (6): 607–621.

U.S. Department of the Army. 2009. “High Acres Landfill- Wetland Mitigation Report”. U.S. Department of the Army.

Underwood, Emma C, Susan L Ustin, and Deanne DiPietro. 2003. “Mapping Nonnative Plants Using Hyperspectral Imagery.” *Remote Sensing of Environment* 86 (2) (July 30): 150–161.

Van Aardt, Jan, and R. H. Wynne. 2001. “Spectral Separability Among Six Southern Tree Species.” *Photogrammetric Engineering and Remote Sensing* 67 (12): 1367–1375.

Yang, Xiaojun. 2005. “Remote Sensing and GIS Applications for Estuarine Ecosystem Analysis: An Overview.” *International Journal of Remote Sensing* 26 (23) (December 10): 5347–5356.

Zedler, Joy B. 2004. “Compensating for Wetland Losses in the United States.” *IBIS* 146 (September 23): 92–100.

Zedler, Joy B., and Suzanne Kercher. 2005. “Wetland Resources: Status, Trends, Ecosystem Services, and Restorability.” *Annual Review of Environment and Resources* 30 (1) (November): 39–74.

Zomer, R J, A Trabucco, and S L Ustin. 2009. “Building Spectral Libraries for Wetlands Land Cover Classification and Hyperspectral Remote Sensing.” *Journal of Environmental Management* 90 (7) (May): 2170–7.

**APPENDIX I: Spectral Reflectance Bands for Electromagnetic Spectrum Regions**

| Spectral Reflectance Bands for Various Wavelength Regions that have Proven to be Useful for Vegetation Analysis | | | | |
|---|---|---|---|---|
| Wavelength Regions (nm) | Description on Electromagnetic Spectrum | Spectral Reflectance Characteristics of Vegetation | Bands | References |
| 400-700 | Visible | Chlorophyll and carotene absorbance (pigments) | 425.4, 436.5, 514.9, 560.1 | (Becker, Lusch, and Qi 2005) |
| | | | 404, 628 | (Schmidt and Skidmore 2003) |
| | | | 550 | (Thenkabail, Smith, and Pauwe 2002) |
| 680-750 | Red Edge | Bio-chemical and bio-physical parameters | 685.5, 731.5, | (Becker, Lusch, and Qi 2005) |
| | | | 675 | (Thenkabail, Smith, and Pauwe 2002) |
| 700-1300 | Near-infrared | Internal leaf structure (useful in discriminating between species) | 812.3, 916.7 | (Becker, Lusch, and Qi 2005) |
| | | | 850, 970, 1240, 1250 | (Rosso, Ustin, and Hastings 2005) |
| | | | 771, 986, | (Schmidt and Skidmore 2003) |
| | | | 720 | (Thenkabail, Smith, and Pauwe 2002) |
| 1300-2500 | Mid-infrared (Short wave-infrared) | Lower reflection due to strong water absorption, minor absorption from bio-chemical content, noise variations due to atmospheric water content | 1398, 1803, 2183 | Schmidt and Skidmore 2003 |

** (Rosso, Ustin, and Hastings 2005)-Data is based on *Salicornia, Scirpus* and *Spartina* salt marsh species

**(Thenkabail, Smith, and Pauwe 2002)- Data is based on estimating crop health

**(Schmidt and Skidmore 2003)- Data is based on salt marsh vegetation

**APPENDIX II: Full Map of RIT Campus**

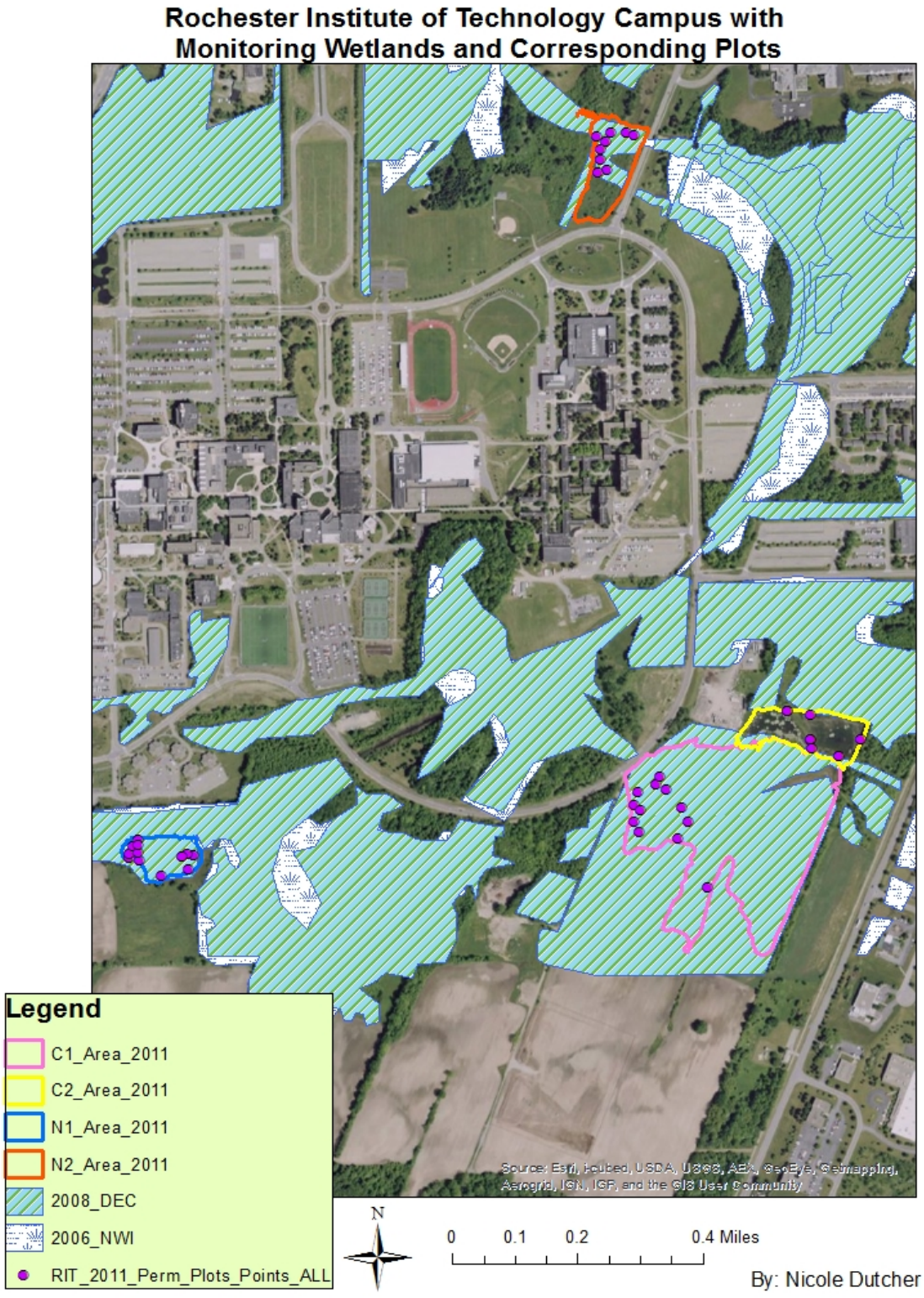

**APPENDIX III: Script for Discriminant Analysis and Linear Discriminant Functions**

```
proc sort data=Wetfield.N2_rawreflec;
by species;
run;


proc stepdisc short slstay=0.005 data=Wetfield.N2_rawreflec;

title2 'Data set = Wetfield.N2_rawreflec';
title3 'This is to discriminate between species';

var W_350-W_1000;
class species;

run;

proc discrim pool=yes listerr crosslisterr data = Wetfield.N2_rawreflec;
class species;

title2 'Discriminant Analysis - Data set = Wetfield.N2_all2';
title3 'Analysis for species';

*variables associated with Wetfield.N2_rawreflec: Species Reflectance 0.0001;
                var W_931 W_934 W_679 W_696 W_639 W_621 W_535;

*variables associated with Wetfield.N2_rawreflec: Species 1st Der 0.001;
*          var WD_949 WD_937 WD_907 WD_876 WD_975 WD_2153 WD_828 WD_2322
WD_859 WD_2252 WD_357;

*variables associated with Wetfield.N2_rawreflec: Species 2nd Der 0.001;
*         var  WDD_876 WDD_881 WDD_2210 WDD_2242 WDD_2032 WDD_866 WDD_949
WDD_943 WDD_1968 WDD_886;

*variables associated with Wetfield.N2_rawreflec: Species Reflectance and both Derivatives
0.005;
*       var WD_933 WDD_609 WD_367 WD_644 WD_363 WD_818;

run;
quit;
```